

TiO₂-modulated tetra(4-carboxyphenyl)porphyrin/perylene diimide organic Z-scheme nano-heterojunctions for efficiently visible-light catalytic CO₂ reduction

Yilin Wang,^a Zhenlong Zhao,^a Rui Sun,^b Ji Bian,^{*a} Ziqing Zhang^{*a} and Liqiang Jing^{*a,b}

^aKey Laboratory of Functional Inorganic Materials Chemistry (Ministry of Education), School of Chemistry and Materials Science, International Joint Research Center for Catalytic Technology, Heilongjiang University, Harbin 150080, P. R. China.

^bKey Lab of Groundwater Resources and Environment of Ministry of Education, Key Lab of Water Resources and Aquatic Environment of Jilin Province, College of New Energy and Environment, Jilin University, Changchun 130012, P. R. China.

*Correspondence: bianji@hlju.edu.cn; zhangzq@hlju.edu.cn; jinglq@hlju.edu.cn

Keywords: perylene diimide nanosheet, tetra(4-carboxyphenyl)porphyrin assembly, Z-scheme heterojunction, TiO₂ energy platform, photocatalytic CO₂ conversion

Experimental section

All of the commercially purchased chemicals and solvents were of analytical grade and without any further purification. Deionized water was used throughout.

Synthesis of TiO₂ nanoparticle. In a typical experiment, a mixture containing 2 mL of butyl titanate and 6 mL of toluene was sonicated for 15 min and further stirred for 15 min to form stable dispersions. A weighing bottle containing the above dispersion was transferred to a Teflon lined stainless-steel autoclave filled with 10 mL deionized water, and kept at 120°C for 6 h. After the system was cooled to room temperature, the white precipitate was collected and washed with ethanol 4 times and dried in an oven at 80°C, then milled into powders with an agate mortar. Finally, the sample was heated in a Muffle furnace at 450°C for 2h to obtain the white powder.

Synthesis of TiO₂ coupled PDI. In a typical synthesis, a proper amount of TiO₂ and PDI were dispersed in 100 mL of ethanol, and ultrasound for 30 min. Then the above mixture was refluxed at 80°C for 3 h. Afterwards, the obtained samples were washed with deionized water several times and dried at 80°C in an oven. This sample was represented as 5T/PDI, which is determined by the mass ratio percentage of TiO₂ to PDI.

Synthesis of 5T&10TP&PDI. 0.1 g PDI, 0.01 g TCPP and 0.005 g TiO₂ were uniformly dispersed in 100 mL of ethanol. Then the mixture was refluxed at 80°C for 3 h. Finally, the obtained sample was washed with deionized water for several times, and dried under vacuum at 80°C overnight. The sample was denoted as 5T&10TP&PDI.

Synthesis of SnO₂ nanocrystal. In a typical procedure, 2.0 g SnCl₄·5H₂O was dissolved in 100 mL deionized water, and then the resulting solution was transferred to a Teflon lined stainless-steel autoclave and heated in an oven at 120°C for 28 h. The product was cooled to room temperature naturally and washed three times with distilled water to remove impurities. The white precipitate was collected by centrifugation, then dried in an oven at 80°C to obtain SnO₂ nanocrystal.

Synthesis of S-TP/PDI heterojunction. In a typical procedure, the 10TP/PDI heterojunction was synthesized as described before, and then the SnO₂ was assembled on it as follows. A proper amount of SnO₂ and 10TP/PDI were dispersed in 50 mL of ethanol and ultrasonicated for 30 min, followed by reflux at 80°C for 3 h. Then, the product was washed with deionized water for 4 times, and drying in a vacuum oven at 80°C.

Preparation of 5T/PDI/10TP and 5T/10TP/PDI electrodes. Both 5T/PDI/10TP and 5T/10TP/PDI were obtained by blade-coating the dispersion of these components on FTO glass in sequence, followed by calcination at 300°C for 30 min in air. In a typical procedure, for 5T/PDI/10TP photoelectrode synthesis, TCPP and TiO₂ were firstly dispersed in a mixture solution of Nafion and ethanol with the volume ratio of 1:9 under vigorous stirring to make individual solution, while PDI was dispersed in a mixture solution of Nafion and H₂O with the volume ratio of 5:8 under vigorous stirring. Then a certain amount of TiO₂ droplets was dropped on a FTO glass

substrate, followed by a blade-coating procedure. Then, the PDI was dispersed on the TiO₂ coated FTO glass, and last the TCPP was dispersed on the substrate. Finally, the sample was calcined at 80°C for 30 min in a muffle furnace, denoted as 5T/PDI/10TP. Similarly, 5T/10TP/PDI electrode was obtained by a same method but with a different coating sequence, swapping PDI and TCPP.

Characterizations

The X-ray powder diffraction (XRD) patterns of the samples were collected by a Bruker D8 advance diffractometer with CuK α radiation. The UV-Vis diffuse reflectance spectra (UV-Vis DRS) of the samples were acquired using Shimadzu UV 2550 spectrophotometer with BaSO₄ as a reference. The Fourier-transform infrared (FT-IR) spectra of the samples were recorded with a Bruker Equinox 55 spectrometer, KBr as the diluents. The morphologies of the samples were analyzed by transmission electron microscopy (TEM) on an FEI Tecnai G2 S-Twin instrument with an acceleration voltage of 200 kV. Atomic force microscopy (AFM) measurements were obtained on a multimode nanoscope VIII instrument (Bruker). The surface photovoltage spectroscopy (SPS) measurements were carried on home-built apparatus, equipped with a lock-in amplifier (SR830, USA) synchronized with a light chopper (SR540, USA). Photoluminescence (PL) measurements were measured by a LS55 Perkin-Elmer fluorescence spectrophotometer at excitation wavelength of 390 nm. Time-resolved surface photovoltage (TR-SPV) measurement was tested at room temperature (in air atmosphere) by using a second harmonic Nd: YAG laser (Lab-130-10H, Newport, Co.) excited by a radiation pulse with 10 ns width. The signal was amplified with a preamplifier and then registered by a 1 GHz digital phosphor oscilloscope (DPO4104B, Tektronix). The Raman spectra were recorded with a Renishaw inVia Confocal Raman spectrometer with a 532 nm laser as the excitation source. The electron paramagnetic resonance (EPR) measurements were carried out on a Bruker EMX plus model spectrometer operating at the X-band frequency. The reactive $\bullet\text{O}_2^-$ species were detected by using 5,5-dimethyl-1-pyrroline N-oxide (DMPO) as a spin trap under visible-light irradiation. The X-ray photoelectron spectroscopy (XPS) was performed by Kratos-Axis ULTRA DLD. Al (Mono) was used as the X-ray source.

Photoelectrochemical and electrochemical measurements. Photoelectrochemical (PEC) and electrochemical reduction measurements were carried out in a traditional three-electrode system. The prepared thin film electrode was used as a working electrode, a platinum plate (99.9%) as the counter electrode, and an Ag/AgCl as the reference electrode. A 0.2 M Na₂SO₄ solution as the electrolyte. High purity nitrogen gas (99.999%) was bubbled through the electrolyte before and during the experiments. PEC experiments were performed in a quartz cell using a 500 W xenon lamp with a cut-off filter ($\lambda > 420$ nm) as the illumination source. An IVIUM V13806 electrochemical workstation was employed to test the photoelectrochemical and electrochemical performance of the series of photocatalysts. All the experiments were performed at room temperature (about 25°C).

Detection of H₂O₂. 25 mg of the catalyst was dispersed in 25 mL of deionized water. The suspension was sonicated for 10 min and stirred for 30 min before the experiment to ensure the high dispersibility. After visible-light irradiation for 2 h, appropriate amount of the

suspension was centrifuged in a 10 mL centrifuge tube. Then 1 mL of 0.1 mol/L potassium hydrogen phthalate ($\text{C}_8\text{H}_5\text{KO}_4$) aqueous solution was added in the supernatant under sonication for 15 min. Afterwards, 1 mL of 0.4 mol/L potassium iodide (KI) aqueous solution was added into the above mixture and kept for 30 min. The H_2O_2 molecules reacted with iodide anions (I^-) under acidic conditions ($\text{H}_2\text{O}_2 + 3\text{I}^- + 2\text{H}^+ \rightarrow \text{I}_3^- + 2\text{H}_2\text{O}$) to produce triiodide anions (I_3^-) possessing a strong absorption at around 350 nm. The amount of I_3^- was determined by means of UV–vis spectroscopy on the basis of the absorbance at 350 nm, from which the amount of H_2O_2 produced was estimated.

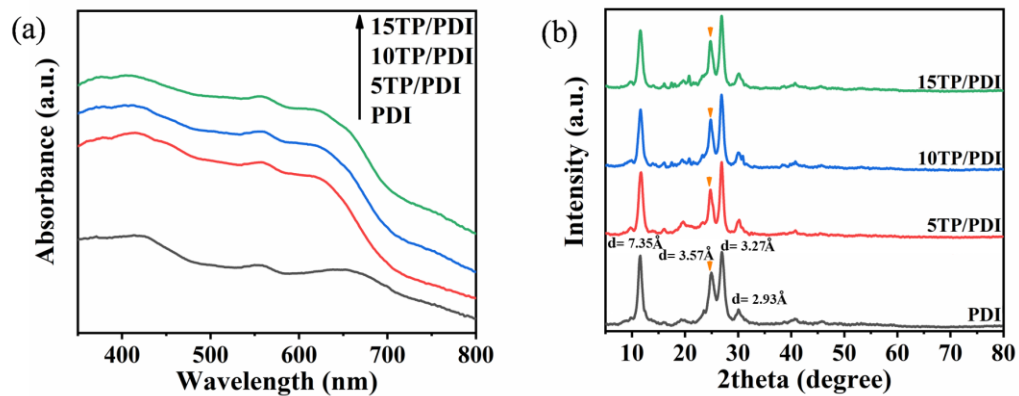


Fig. S1 (a) DRS spectra and (b) XRD patterns of PDI and xTP/PDI heterojunctions.

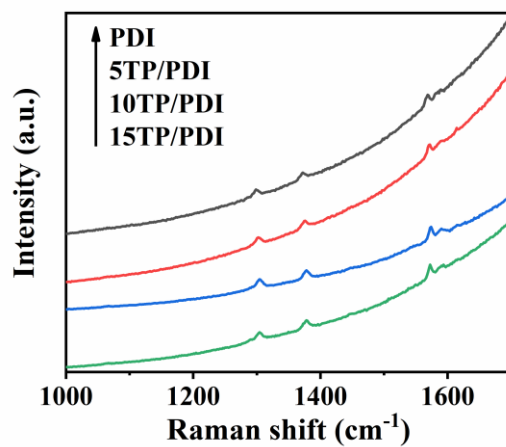


Fig. S2 Raman spectra of PDI and xTP/PDI heterojunctions.

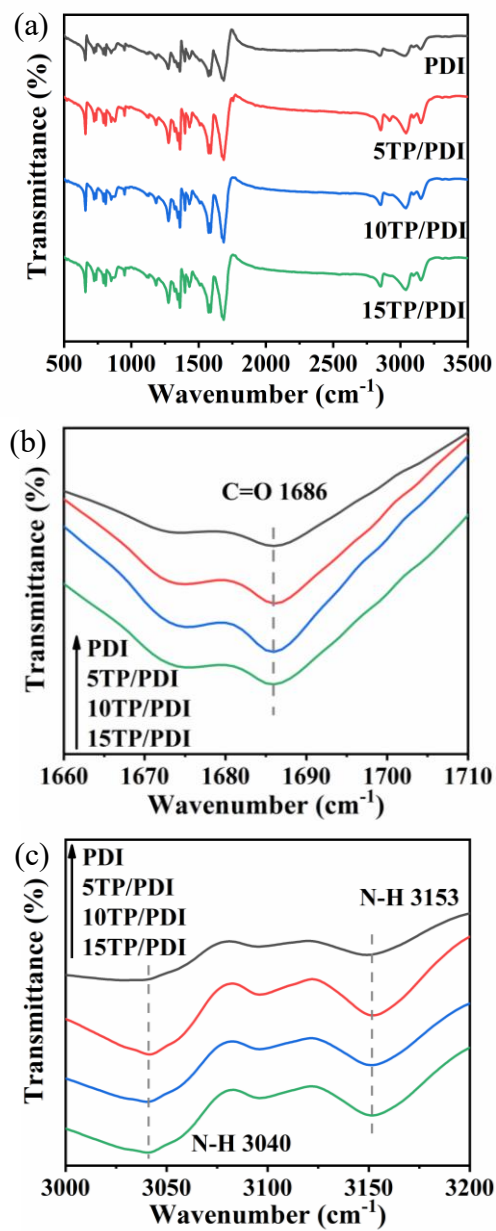


Fig. S3 (a) FT-IR spectra of PDI and xTP/PDI heterojunctions. (b, c) The enlarged view of FT-IR spectra for the C=O and N-H vibration peaks.

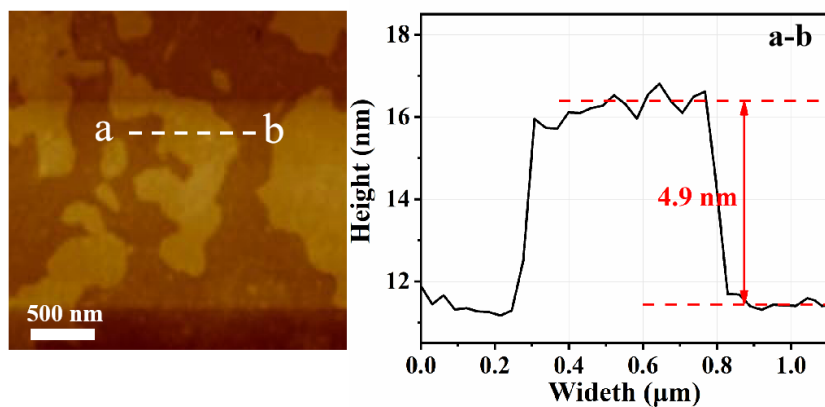


Fig. S4 AFM image and the corresponding height profile of PDI.

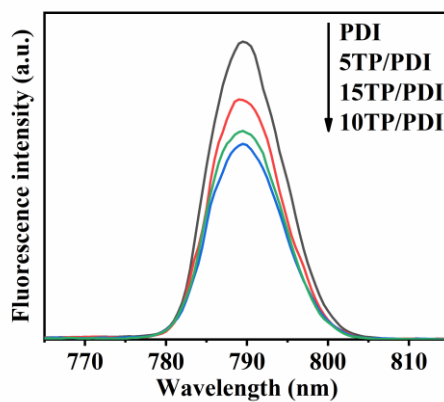


Fig. S5 PL spectra of PDI and xTP/PDI heterojunctions.

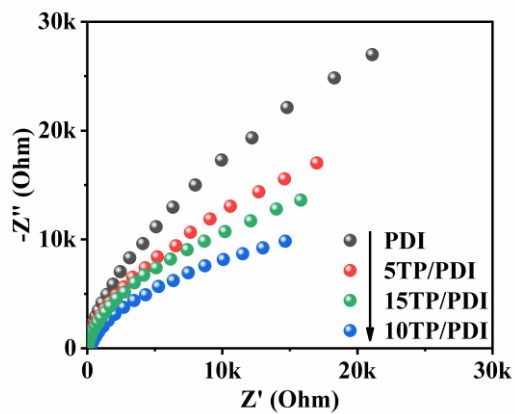


Fig. S6 EIS spectra of PDI and xTP/PDI heterojunctions.

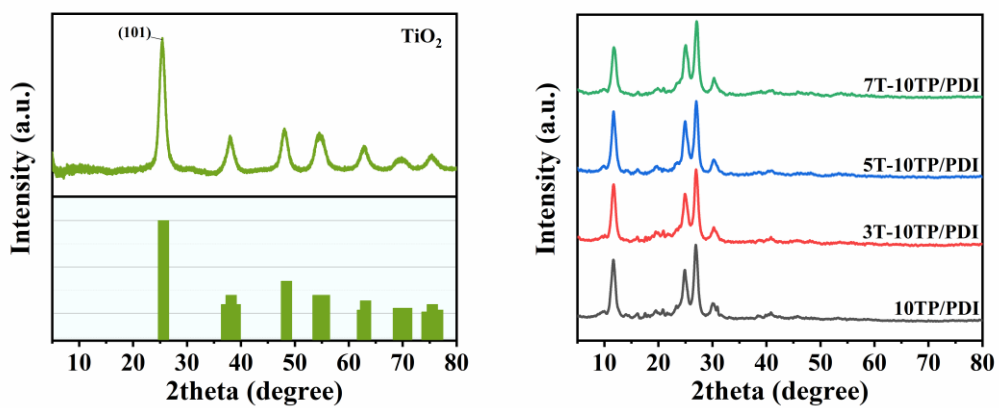


Fig. S7 XRD patterns of (a) TiO_2 and (b) 10TP/PDI and $y\text{T-10TP/PDI}$ heterojunctions.

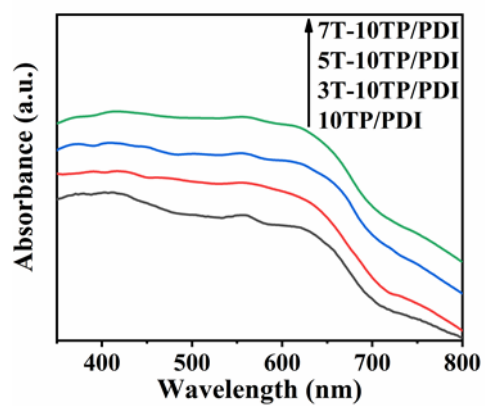


Fig. S8 DRS spectra of 10TP/PDI and γ T-10TP/PDI heterojunctions.

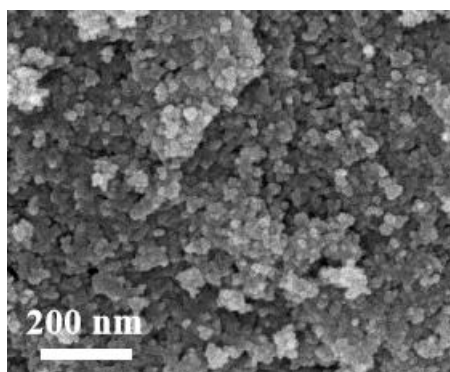


Fig. S9 TEM image of TiO_2 nanoparticles.

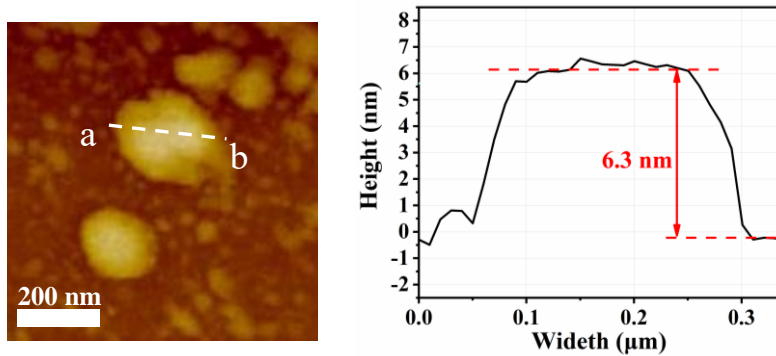


Fig. S10 AFM image and the corresponding height profile of 5T-10TP/PDI heterojunction.

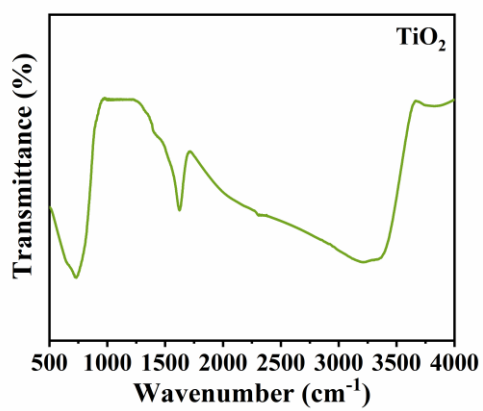


Fig. S11 FT-IR spectrum of TiO₂ nanoparticle.

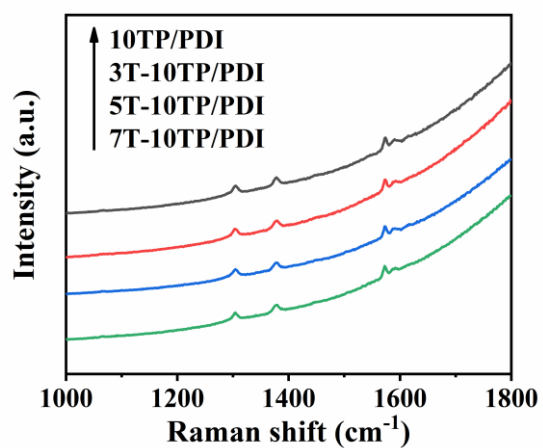


Fig. S12 Raman spectra of 10TP/PDI and γ T-10TP/PDI heterojunctions.

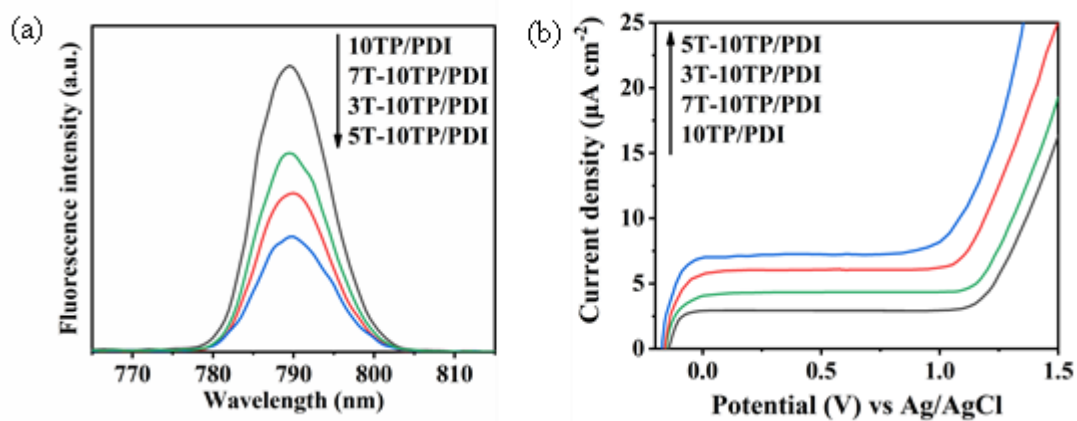


Fig. S13 (a) PL spectra and (b) Photoelectrochemical I-V curves of 10TP/PDI and γ T-10TP/PDI heterojunctions.

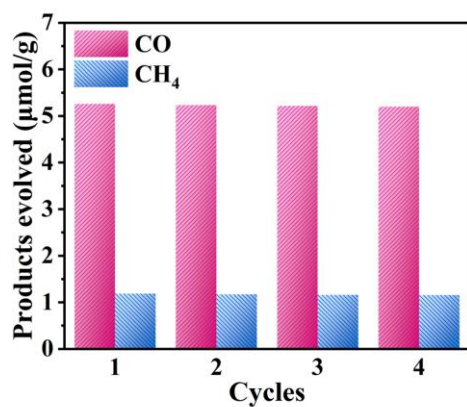


Fig. S14 Photocatalytic cycling test for CO₂ reduction over 5T-10TP/PDI heterojunction.

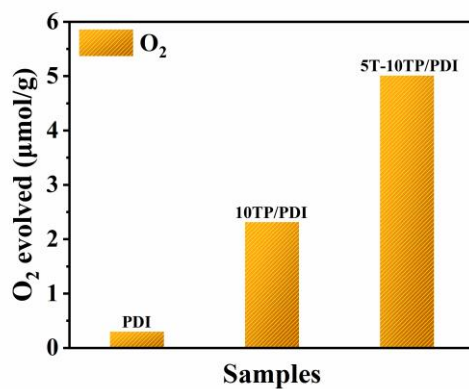


Fig. S15 The evolved O₂ during CO₂ photoreduction of PDI, 10TP/PDI and 5T-10TP/PDI heterojunction.

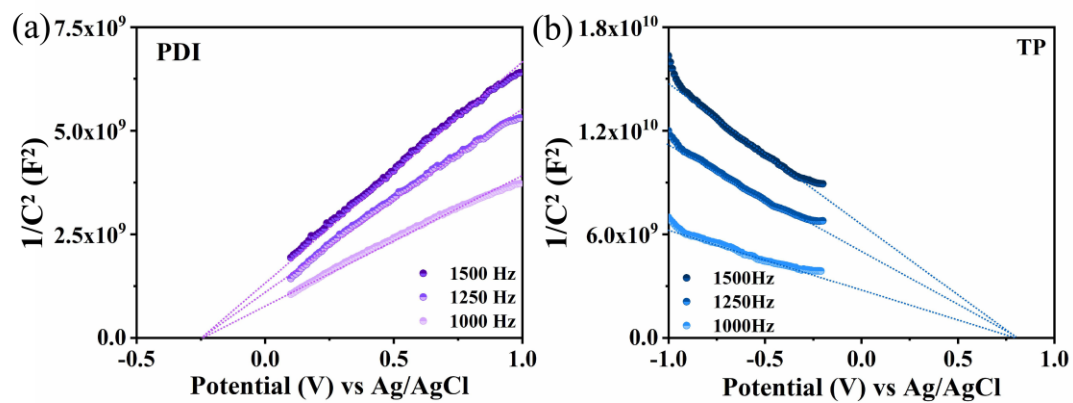


Fig. S16 Mott–Schottky curves of (a) PDI and (b) TP at different frequencies.

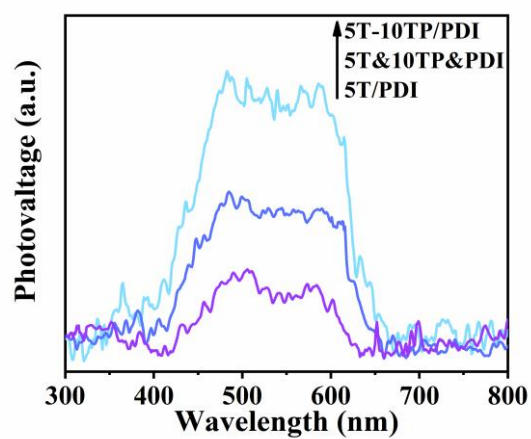


Fig. S17 SPS spectra of 5T-10TP/PDI, 5T&10TP&PDI and 5T-PDI.

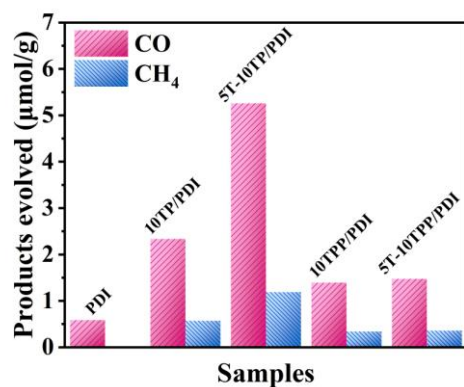


Fig. S18 Photocatalytic activities for CO₂ reduction of PDI, 10TP/PDI, 5T-10TP/PDI, 10TPP/PDI and 5T-10TPP/PDI.

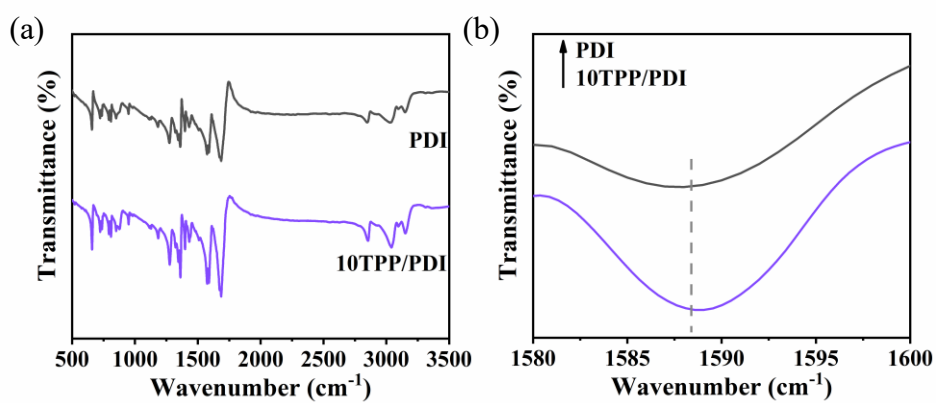


Fig. S19 FT-IR spectra (a) and the enlarged view (b) of PDI and 10TPP/PDI heterojunction.

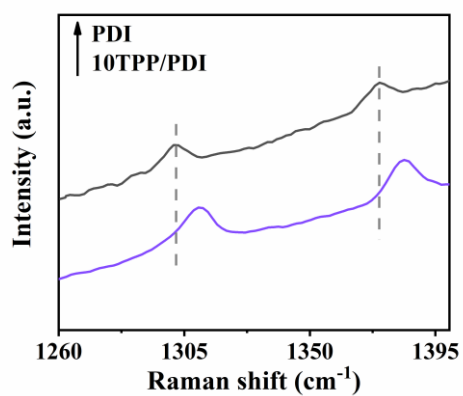


Fig. S20 Raman spectra of PDI and 10TPP/PDI.

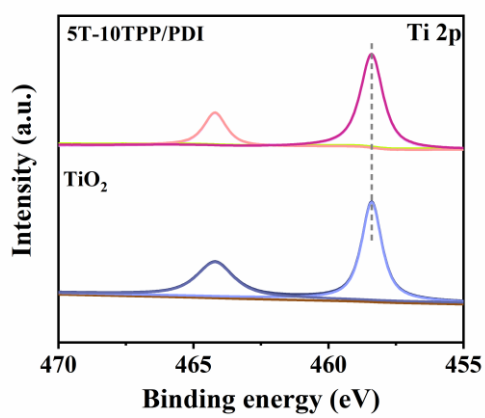


Fig. S21 XPS spectra of Ti 2p for TiO₂ and 5T-10TPP/PDI.

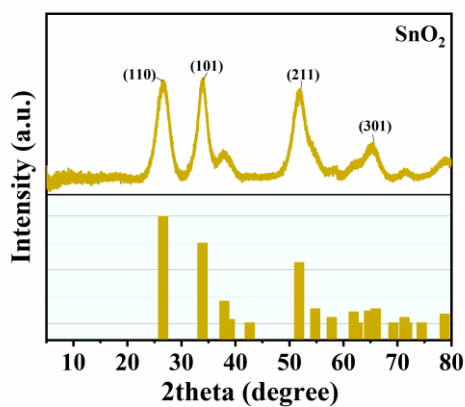


Fig. S22 XRD pattern of SnO₂.

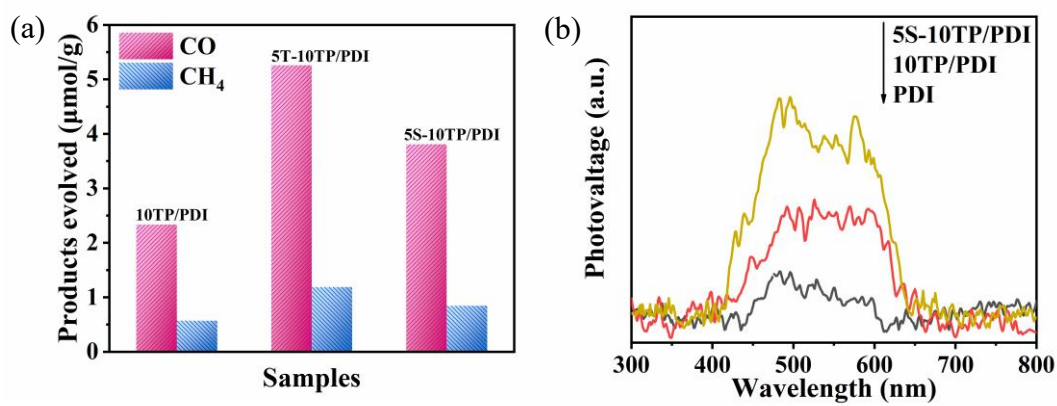


Fig. S23 (a) Photocatalytic activities for CO₂ reduction and (b) SPS spectra of 10TP/PDI, 5T-10TP/PDI and 5S-10TP/PDI heterojunction.